PHOTOSYNTHETICA
International Journal for Photosynthesis Research

DOI 10.32615/ps.2022.024 PHOTOSYNTHETICA 60 (3): 376-388, 2022

Biochemical, gas exchange, and chlorophyll fluorescence analysis of maize genotypes under drought stress reveals important insights into their interaction and homeostasis

G.M. SINGH[*,**], S. GOLDBERG[**,***,#], D. SCHAEFER[**,#], F. ZHANG[*,##,+], S. SHARMA[###], V.K. MISHRA[###], and J. XU[**,***,#,+]

MARA-CABI Joint Laboratory for Biosafety, Institute of Plant Protection, Chinese Academy of Agricultural Sciences, 100193 Beijing, China[*]
Centre for Mountain Futures (CMF), Kunming Institute of Botany, 650201 Kunming, Yunnan, China[**]
East and Central Asia Regional Office, World Agroforestry, 650201 Kunming, Yunnan, China[***]
CAS Key Laboratory for Plant Diversity and Biogeography of East Asia, Kunming Institute of Botany, Chinese Academy of Sciences, 650201 Kunming, Yunnan, China[#]
College of Agriculture and Ecological Engineering, Hexi University, Zhangye, 734000 Gansu, China[##]
Department of Genetics and Plant Breeding, Banaras Hindu University, 221005 Varanasi, India[###]

Abstract

Many studies have been conducted on maize to study the effect of drought on yield at the flowering stage, but understanding biochemical and photosynthetic response against drought at the seedling stage needs to be well established. Thus, to understand differential changes and interaction of biochemical and photosynthetic parameters at the seedling stage under drought, a greenhouse experiment with twelve maize genotypes under severe drought (30% field capacity) and irrigated (90–100% field capacity) conditions were performed. Drought differentially altered biochemical and photosynthetic parameters in all genotypes. A sharp increase in hydrogen peroxide, malondialdehyde (MDA), and total antioxidant capacity (TAOC) were seen and a positive association between H_2O_2 and TAOC, and MDA and transpiration rate (E) was observed under drought. Nonphotochemical quenching increased under drought to avoid the photosystem damage. PCA biplot analysis showed that reducing E and increasing photosynthetic efficiency would be a better drought adaptation mechanism in maize at the seedling stage.

Keywords: chlorophyll fluorescence; drought; gas exchange; interaction; maize.

Highlights

- Stomatal and nonstomatal limitations of photosynthesis occur in maize under severe drought
- A strong positive association was found between H_2O_2 and TAOC
- Reducing E and increasing F_v/F_m would be a better drought adaptation mechanism

Received 21 November 2021
Accepted 25 April 2022
Published online 3 June 2022

[+]Corresponding authors
e-mail: jxu@mail.kib.ac.cn
f.zhang@cabi.org

Abbreviations: APX – ascorbate peroxidase; ASH – ascorbate; ATP – adenosine triphosphate; CAT – catalase; Chl – chlorophyll; C_i/C_a – the ratio of intercellular to ambient CO_2 concentration; DAS – days after sowing; E – transpiration rate; F_v/F_m – maximal quantum efficiency of PSII; g_{H2O} – water vapor conductance; GPX – glutathione peroxidase; GSH – glutathione; GST – glutathione S-transferase; MDA – malondialdehyde; NPQ – nonphotochemical quenching; $O_2^{\bullet-}$ – superoxide radical; $^1O_2$ – singlet oxygen; $^{\bullet}OH$ – hydroxyl radical; PETC – photosynthetic electron transport chain; P_N – net assimilation rate; ROS – reactive oxygen species; SOD – superoxide dismutase; TAOC – total antioxidant capacity; VPD – air to leaf vapor pressure deficit; VWC – volumetric water content; Y_{NPQ} – quantum yield of NPQ-related energy loss; Φ_{PSII} – quantum yield of photosynthetic electron transport.

Acknowledgments: We sincerely acknowledge the Yunnan Academy of Agricultural Sciences (YAAS), Yunnan, Honghe Hani, and Yi Autonomous Prefecture Academy of Agricultural Sciences, Yunnan, China for providing the maize genotypes used in the study. We are also thankful to the Center for Mountain Futures (CMF), Yunnan, China, the Center for Agriculture and Biosciences International (CABI), and Kunming Institute of Botany (KIB), Yunnan, China for their valuable support and resources. This research was partly funded by China's donation to the CABI Development Fund and Gansu Provincial Department of Education Industry Support Programme (2021CYZC-53). Feng Zhang was supported by CABI with core financial support from its member countries (*see* https://www.cabi.org/what-we-do/how-we-work/cabi-donors-and-partners/).
Conflict of interest: The authors declare that they have no conflict of interest.

Introduction

Maize (*Zea mays* sp.) is widely used as food, feed, and biofuel around the world. Its yield is hugely limited by drought in various parts of the world. Though maize has higher productivity compared to other cereals, its productivity is greatly limited by biotic and abiotic stresses (Assefa and Ayalew 2019). Around 40% of Africa's maize-growing area faces occasional drought stress, resulting in yield losses of 10–25%, while 25% of the maize crop suffers frequent drought, with losses of up to half (Fisher *et al.* 2015). Fifty years of meteorological and annual yield data (1958–2007) of the United States of America estimated that drought caused 13% of the USA's maize and soybean yield variability (Zipper *et al.* 2016). Drought interferes with plant growth, nutrient accumulation, water relations, and photosynthesis, thus reducing the yield (Farooq *et al.* 2009, Praba *et al.* 2009). Accordingly, plants have developed well sensing and signal transduction systems to respond to water limitation and osmotic stress (Bhaskara *et al.* 2012). Oxidative signaling is one of the major network complexes that operates under water-limiting conditions despite regulating plant growth and development under normal conditions (Tsukagoshi *et al.* 2010, Noctor *et al.* 2014). It generally happens through the reactive oxygen species (ROS) network which includes, hydrogen peroxide (H_2O_2), superoxide radical ($O_2^{\bullet-}$), singlet oxygen ($^1O_2$), and the hydroxyl radical ($^{\bullet}OH$). Under ambient growth conditions, ROS are produced continuously in the plants (Jakob and Heber 1996), and usually $^1O_2$ and $^{\bullet}OH$ production is kept at a minimum, while H_2O_2 and $O_2^{\bullet-}$ production is kept at a higher rate (Noctor and Foyer 1998). They function as various signaling molecules and participate under diverse stimuli (Singh *et al.* 2019). Generally, due to the photosynthesis and respiration process, ROS generations are inevitable and are mainly produced in chloroplasts, mitochondria, and peroxisomes.

The leakage of electrons from the photosynthetic electron transport chain (PETC) leads to the formation of ROS, particularly singlet oxygen [by energy transfer from triplet excited state chlorophyll (Chl) to O_2] and hydrogen peroxide (by reduction of O_2 through Mehler reaction) (Mehler 1951, Asada and Takahashi 1987). Mainly these ROS are highly unstable causing significant damage to DNA, cell membranes, proteins, and lipids by unrestricted oxidation, if not controlled or scavenged properly (Richter and Schweizer 1997, Dat *et al.* 2000, Apel and Hirt 2004). To avoid the cytotoxic effect of ROS, the plant has developed various scavenging mechanisms, which mainly operated through enzymatic (superoxide dismutase, SOD; ascorbate peroxidase, APX; glutathione peroxidase, GPX; glutathione S-transferase, GST; catalase, CAT) and nonenzymatic (ascorbate, ASH; glutathione, GSH; alpha-tocopherol; carotenoids and flavonoids) scavenging systems (Mittler *et al.* 2004, Gill and Tuteja 2010). But during abiotic stress, especially during drought, the redox homeostasis balance breaks down due to increased and uncontrolled production of ROS (Sgherri *et al.* 1993, Smirnoff 1993, Boo and Jung 1999, Polle 2001), creating an imbalance in ROS production and scavenging. Mostly during water stress, initial signaling from abscisic acid from roots to shoot (Zhang and Davies 1987, Davies and Zhang 1991) leads to the closing of stomata to reduce transpiration flux, which in turn declines the CO_2 intake leading to higher leakage of electrons from PETC to O_2 by the Mehler reaction (Smirnoff 1993, Dat *et al.* 2000). Further, the reduced CO_2 fixation decreases the consumption of ATP and NADPH, which in turn reduces $NADP^+$ (major electron acceptor in PSI) regeneration through the Calvin cycle. This provokes the over-reduction of the photosynthetic electron transport chain (Cruz de Carvalho 2008) and leakage of electrons to molecular oxygen thus producing higher amount of H_2O_2 (Asada 1999), leading to drought-induced oxidative stress.

In addition to cell damage, drought-induced oxidative stress impairs the photosystem machinery of the plant by creating the disequilibrium between light capture and utilization (Mattos and Moretti 2015), hence reducing photosynthetic efficiency. Usually, under drought-induced reduced CO_2 fixation, the rate of absorption of light energy by photosynthetic pigments exceeds the rate of its consumption in chloroplasts, hence the absorbed light energy accelerates the process of photoinhibition (inhibition of PSII repair). Further, during drought, the CO_2 assimilation rate showed a decrease due to stomatal and nonstomatal limitations (Cossins and Chen 1997). Additionally, drought not only reduces stomatal conductance and diffusion of CO_2 but also decreases ribulose-1,5-bisphosphate (RuBP) generation, ATP synthesis, and other vital metabolic processes (Cossins and Chen 1997). Chl fluorescence is one of the most prominent approaches used to study the photosynthetic efficiency of plants (Murchie and Lawson 2013). F_v/F_m (maximal quantum efficiency of PSII) ratio is a key parameter to detect the PSII photoinhibition induced by stress (Krause and Weis 1991).

Maize as a C_4 plant fixes CO_2 more efficiently by reducing photorespiration but it is very sensitive to drought at various stages of development (Sinclair *et al.* 1990, Farré *et al.* 2000). Many studies have been done at the anthesis stage to understand the effect of drought on yield and other agronomic traits, but knowledge of the differential response of biochemical and photosynthetic traits and their interaction is limited and need to be well explored. This present study aims at studying how maize responds to drought at the seedling stage through biochemical and photosynthetic changes and how they interact with each other, which could help in selecting the best physiologically adapted genotype for drought. Based on these observed parameters HD-6 genotype relatively performed well under drought compared to others.

Materials and methods

Plant growth conditions and drought treatments: Twelve genotypes were used in the present study (text table). Seeds were surface-sterilized with sodium hypochlorite (3%) for 10 min and sown in a 30 × 30 cm pot filled with well-mixed sandy loam soil. Each pot

was inoculated with 7 g (300 spores g^{-1}) *Rhizhopagus irregularis*, arbuscular mycorrhiza formulation powder. Fertilizers were applied according to soil nutrient analysis and plants were grown under optimum growth conditions in a greenhouse at the Kunming Institute of Botany, Yunnan, China from 2019 to 2020. The average day/night temperature of the greenhouse was 29.5/20°C and relative humidity was 55–80% throughout the growth period.

No.	Genotype	Source
1	GJ-3	Local cultivar
2	JH-19A-501-36	YAAS-CIMMYT
3	YS-18B-150-44	YAAS-CIMMYT
4	GJ-14	Local cultivar
5	JH-19A-501-23	YAAS-CIMMYT
6	GJ-2	Local cultivar
7	La-posta-seq	YAAS-CIMMYT
8	JL-118	Local cultivar
9	YS-18B-150-43	YAAS-CIMMYT
10	HD-6	Local cultivar
11	JH-18A-514-38	YAAS-CIMMYT
12	GJ-1	Local cultivar

Before the initiation of the experiment, a pre-soil analysis was done to find out a field capacity (FC) of the soil. Soil (of bulk density 1.45 g cm^{-3}) used for the experiment was filled in the same pots used for the experiment and saturated fully. After 24 and 48 h of saturation, soil moisture was measured by an *SM150T* soil moisture sensor (*Delta-T Devices Ltd*., United Kingdom). After 24 h, the volumetric water content (VWC) was averaged at 20.8%, and after 48 h, it was 18%. Soil moisture content after 2–3 d after irrigation or saturation has been generally considered as field capacity (Veihmeyer and Hendrickson 1931, Kirkham 2005). Thus 18% VWC was considered moisture at FC and 5–5.5% VWC (30% of FC) was regarded as severe drought stress. The experiment was arranged in a combined block design (CBD) containing two treatments, *i.e.*, control (90–100% FC) and drought (30% FC) with 15 plants per genotype per treatment. Each pot was sown with two seeds and thinned to one at 14 d after sowing (DAS). Drought treatment was initiated at 21 DAS and brought soil moisture content to 30% FC (13–15 d after stress initiation) and all observations and sampling were taken simultaneously. Drought treatment was monitored daily by *Delta 150* soil moisture meter. Leaf (top, the most fully expanded) samples from five biological replicates from all treatments were harvested and frozen immediately in liquid nitrogen and later stored in a –80°*C* freezer for biochemical analysis.

Malondialdehyde (MDA) and reactive oxygen species assay: Fresh leaf tissue were homogenized with phosphate buffer to prepare a 10%-aliquot solution and used for following bioassays in triplicate with required dilutions. MDA was measured to detect the rate of lipid peroxidation in maize leaves by the thiobarbituric acid reactive substances (TBARS) assay method using the MDA assay kit (*A003-3*) obtained from *Nanjing Jiancheng Bioengineering Institute* (http://www.njjcbio.com/), China. In principle, thiobarbituric acid reacts with MDA to generate a red compound that has the maximum absorbance at 532 nm; the method was used with minor modifications and expressed as nmol ml^{-1} of homogenate (Heath and Packer 1968, Dhindsa *et al.* 1981). Hydrogen peroxide (H_2O_2) content was estimated using commercial kit *A064-1* manufactured and supplied by *Nanjing Jiancheng Bioengineering Institute*, China, based on the principle of its reaction with molybdate to form coordination complex and recording its absorbance at 405 nm in spectrophotometer plate reader. The amount of H_2O_2 was calculated according to the user manual formula of the kit with little modifications and expressed as µmol(H_2O_2) 0.1 ml^{-1} of homogenate.

Total antioxidative capacity (TAOC): Production of total enzymatic [superoxide dismutase (SOD), glutathione peroxidase (GPX), catalase (CAT), glutathione S-transferase (GST), *etc*.] and nonenzymatic (vitamins, amino acids, and metalloproteins) antioxidants were estimated by commercial *A015* kit produced and supplied by *Nanjing Jiancheng Bioengineering Institute*, China. The kit is based on the principle that antioxidative compounds can reduce Fe^{3+} to Fe^{2+}, and Fe^{2+} reacts with phenanthroline to produce a stable complex, which was measured at 520 nm to calculate TAOC and expressed as U 0.1 ml^{-1} of homogenate.

Photosynthesis and Chl fluorescence measurements: Gas exchange and Chl fluorescence were measured in the youngest fully expanded leaf using a portable gas-exchange fluorescence system (*GFS-3000* and *PAM-Fluorometer 3056-FL*, *Heinz Walz GmbH*, Germany). Gas exchange was measured between 9:00–11:00 h by setting an absolute CO_2 concentration of 400 ppm, relative humidity of 75%, cuvette temperature of 25°*C,* and PAR of 1,500 µmol(photon) m^{-2} s^{-1}. A light-response curve was calculated for both drought and control plants and found constant at PAR of 1,500 µmol(photon) m^{-2} s^{-1}. Assimilation rate (P_N), transpiration rate (E), water vapor conductance (g_{H2O}), and intercellular CO_2 concentration (C_i) were calculated according to von Caemmerer and Farquhar (1981). Chl fluorescence parameters maximal quantum efficiency of PSII (F_v/F_m), quantum yield of photosynthetic electron transport [$\Phi_{PSII} = (F_m' - F)/F_m'$], nonphotochemical quenching [$NPQ = (F_m - F_m')/F_m'$], and quantum yield of NPQ-related energy loss [$Y_{NPQ} = (F/F_m') - (F/F_m)$] were calculated from the Chl fluorescence measurement according to Genty *et al*. (1989) and Baker (2008). All the Chl fluorescence measurements were done before dawn (dark-adapted) by exposing them to strong actinic light.

Statistical analysis: The means were compared between control and drought by two-way analysis of variance (*ANOVA*) and *Tukey*'s post-hoc test, with p=0.05 significance level. The positive relative or delta change

was calculated by subtracting values under control with drought or *vice versa* (whichever is applicable) and were divided by control values except for TAOC and were ranked from the lowest to the highest. Lower delta change suggests that lesser difference between control (C) and drought (T, treatment), and is considered a better performer for that respective trait. While for TAOC relative or delta change was calculated by subtracting values under drought with control and ranked from the highest to lowest value, indicating higher TAOC under drought is essential for a plant to scavenge ROS and avoid cellular damage. *Pearson*'s correlation (two-tailed) and principal component analysis (PCA) biplot analysis for both genotypes and recorded parameters was performed in *Origin Pro 2022* (https://www.originlab.com/).

Results

Hydrogen peroxide: The H_2O_2 content drastically increased due to drought in all genotypes (Fig. 1*A*). Under control, GJ-2 showed the highest H_2O_2 followed by GJ-1 and the least amount found in JH-18A-514-38, while in drought-treated samples, the highest H_2O_2 was found in GJ-2 followed by GJ-3 while the least was found in YS-18B-150-43 and YS-18B-150-44. The positive delta change [(T – C)/C] was the lowest in GJ-1 followed by JH-19A-501-36 and highest in JH-18A-514-38 (Table 1). Genotypes were ranked according to a positive delta (from the lowest to the highest) for their comparison and interpretation. The delta change shows the relative decrease or increase of the value of the parameter in drought compared to its respective control. Further, under drought, H_2O_2 showed a higher variation than that of control (Table 2). A summary of the mean and standard deviation (SD) of the measured parameters is presented in Table 2.

Total antioxidants capacity: The TAOC significantly increased in all genotypes under drought except JH-19A-501-23, JL-118, and GJ-1 (very marginal reduction was seen under drought) (Fig. 1*B*). Genotypes HD-6 and GJ-2 had the highest TAOC in control, whereas JL-118 was the lowest. Similarly HD-6 contained the highest TAOC in drought followed by GJ-2 and the lowest was seen in JL-118. Genotypes were ranked based on treatment–control (T–C) from the highest to lowest (Table 1). The highest TAOC content genotypes under drought may be considered good oxidative stress-balancing lines.

Malondialdehyde: Drought conditions significantly increased MDA content (Fig. 1*C*). Genotype JH-19A-501-23 contained the highest MDA followed by YS-18B-150-43 and the least in La-posta-seq in control, while under drought, GJ-3 had a higher MDA followed by YS-18B-150-43 and the least in La-posta-seq. The positive delta change [(T – C)/C] was lowest in JH-19A-501-23 followed by HD-6 and the highest in GJ-3 (Table 1). Genotypes were ranked according to positive delta (the lowest to the highest). Lower delta change is supposed to be more tolerant to drought.

Net assimilation rate (P_N): The P_N was significantly reduced in all genotypes under drought (Fig. 2*D*). All genotypes significantly differed under control for P_N, but not in drought. GJ-14 had the highest P_N followed by YS-18B-150-43 and the lowest in La-posta-seq under control, while under drought, YS-18B-150-43 showed the highest P_N followed by YS-18B-150-44 and the lowest in GJ-2. However, HD-6 and JL-118 exhibited the lowest and highest positive delta change [(C – T)/C], respectively (Table 1).

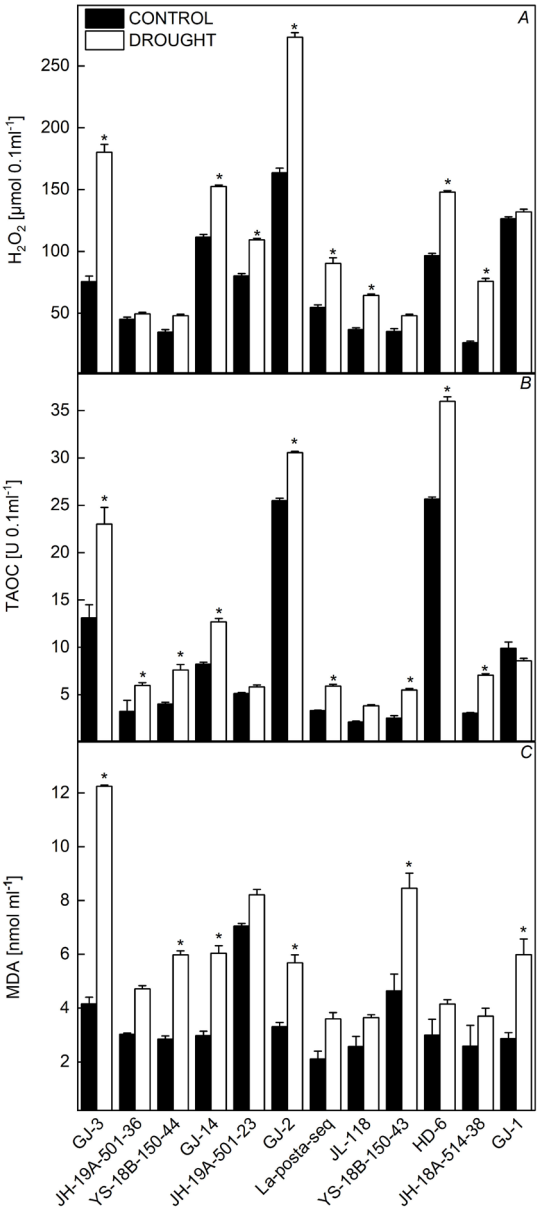

Fig. 1. Changes in (*A*) hydrogen peroxide (H_2O_2), (*B*) total antioxidant capacity (TAOC), and (*C*) malondialdehyde (MDA) content in different maize genotype leaves in a greenhouse experiment. Values are means ± SE, $n = 5$. * indicates significant differences at $P<0.05$.

Table 1. Ranking of genotypes based on their relative or delta change of measured parameters under drought (D) and control (C). All traits except TAOC are ranked from the lowest to the highest delta change values, while TAOC are ranked from the highest to lowest. Genotypes that showed lower delta change (less difference between control and drought) except for TAOC, were considered better performers for that respective trait. However, higher TAOC under drought compared to control is considered a better performer. HD-6 (bold) performed comparatively well under drought.

Rank	H_2O_2	MDA	TAOC	E	VPD	g_{H2O}	P_N	C_i/C_a	F_v/F_m	Φ_{PSII}	NPQ	Y_{NPQ}
	(T – C)/C	(T – C)/C	T – C	(C – T)/C	(T – C)/C	(C – T)/C	(C – T)/C	(T – C)/C	(C – T)/C	(C – T)/C	(T – C)/C	(T – C)/C
1	GJ-1	JH-19A-501-23	**HD-6**	JH-19A-501-23	JH-19A-501-23	JH-19A-501-23	**HD-6**	**HD-6**	**HD-6**	**HD-6**	JH-19A-501-23	YS-18B-150-43
2	JH-19A-501-36	**HD-6**	GJ-3	GJ-3	**HD-6**	GJ-3	JL-118	YS-18B-150-43	JH-18A-514-38	JH-19A-501-23	YS-18B-150-43	JH-19A-501-23
3	YS-18B-150-43	JL-118	GJ-2	JH-19A-501-36	JL-118	JH-19A-501-36	YS-18B-150-44	JH-19A-501-36	YS-18B-150-43	GJ-1		**HD-6**
4	JH-19A-501-23	JH-18A-514-38	GJ-14	JL-118	JH-19A-501-36	**HD-6**	YS-18B-150-43	La-posta-seq	YS-18B-150-43	JH-19A-501-36	GJ-14	GJ-1
5	GJ-14	JH-19A-501-36	JH-18A-514-38	YS-18B-150-44	YS-18B-150-44	JL-118	JH-19A-501-23	GJ-2	GJ-2	JH-18A-514-38	**HD-6**	JH-18A-514-38
6	YS-18B-150-44	GJ-2	YS-18B-150-44	YS-18B-150-43	GJ-1	YS-18B-150-43	GJ-3	JH-19A-501-23	JH-19A-501-23	GJ-2	GJ-3	GJ-14
7	**HD-6**	La-posta-seq	YS-18B-150-43	**HD-6**	GJ-14	JH-18A-514-38	La-posta-seq	GJ-14	YS-18B-150-44	GJ-14	JH-18A-514-38	JH-19A-501-36
8	La-posta-seq	YS-18B-150-43	JH-19A-501-36	GJ-2	GJ-2	GJ-2	JH-19A-501-36	GJ-1	GJ-1	YS-18B-150-44	JH-19A-501-36	GJ-3
9	GJ-2	GJ-14	La-posta-seq	GJ-14	GJ-3	YS-18B-150-44	GJ-1	JH-19A-501-36	GJ-14	GJ-1	YS-18B-150-44	GJ-2
10	JL-118	GJ-1	JL-118	GJ-1	YS-18B-150-43	La-posta-seq	GJ-14	JH-18A-514-38	JL-118	GJ-3	GJ-2	YS-18B-150-44
11	GJ-3	YS-18B-150-44	JH-19A-501-23	La-posta-seq	JH-18A-514-38	GJ-1	JH-18A-514-38	JL-118	GJ-3	JL-118	La-posta-seq	La-posta-seq
12	JH-18A-514-38	GJ-3	GJ-1	JH-18A-514-38	La-posta-seq	GJ-14	GJ-2	GJ-3	La-posta-seq	La-posta-seq	JL-118	JL-118

Air to leaf vapor pressure deficit (VPD): The VPD was calculated according to von Caemmerer and Farquhar (1981) based on intercellular H_2O mole fraction within the leaf (ppm)(w_i) and H_2O mole fraction in the cuvette (ppm) (w_a) and expressed as Pa kPa^{-1}. The formula for VPD calculated by default in *GFS-3000*, VPD = $(w_i – w_a)/[1 – (w_i + w_a/2)]$. VPD increased in all genotypes under drought compared to control. The variation for VPD was found to be higher in drought condition between genotypes compared to control (Fig. 2*B*, Table 2). Under control, JL-118 showed the highest VPD followed by JH-18A-514-38 and the lowest was in GJ-2, similarly under drought, JH-18A-514-38 had the highest VPD followed by La-posta-seq and the lowest was in GJ-2. The positive delta change [(T – C)/C] was the lowest in JH-19A-501-23, followed by HD-6, and the highest was in La-posta-seq (Table 1).

The ratio of intercellular to ambient CO_2 (C_i/C_a): The C_i/C_a ratio was used to evaluate stomatal acclimation (Sage 1994). All genotypes varied under both control and drought for C_i/C_a ratio (Fig. 2*E*). Genotype GJ-2 showed a higher C_i/C_a ratio followed by GJ-14 and the lowest in GJ-3 under control, while in drought, GJ-14 showed the highest followed by JH-19A-501-36 and the lowest in YS-18B-150-43. The lowest and highest positive delta change [(T – C)/C] was seen in HD-6 and GJ-3, respectively (Table 1).

Transpiration rate (E): Transpiration was reduced significantly under drought. Significant variation was found in transpiration between genotypes in both control and drought (Fig. 2*A*). Genotype GJ-14 showed the highest E, followed by JH-18A-514-38, and the lowest in GJ-1 in control, while under drought, JH-19A-501-23 had the highest E, followed by GJ-3, and the lowest was in GJ-1. The positive delta change [(C – T)/C] was the lowest in JH-19A-501-23, followed by GJ-3, and the highest was in JH-18A-514-38, and all the genotypes were ranked from the lowest to the highest (Table 1).

Water vapor conductance (g_{H2O}): Significant variation was found for g_{H2O} between genotypes under both control and drought. It decreased significantly under drought compared to control (Fig. 2*C*). Genotype GJ-14 showed the highest g_{H2O} followed by GJ-2 and the lowest was seen in JH-18A-514-38 under control, while in drought, JH-19A-501-23 showed the highest g_{H2O} followed by JH-19A-501-36 and the lowest in JH-18A-514-38. Similarly, JH-19A-501-23 and GJ-14 exhibited the lowest and highest positive delta change [(C – T)/C], respectively (Table 1).

Maximal quantum efficiency of PSII (F_v/F_m): The F_v/F_m ratio differed considerably between control and drought (Fig. 3*A*). Generally, F_v/F_m ranges from 0 to 0.84. Genotype GJ-14 showed higher F_v/F_m followed by GJ-3 and the least by HD-6 under control, while in drought, it ranged from 0.638 (La-posta-seq) to 0.77 (YS-18B-150-43). The lowest and highest positive delta change [(C – T)/C]

Table 2. Mean and standard deviation (SD) of the measured parameters under control and drought. C_i/C_a – the ratio of intercellular to ambient CO_2 concentration; E – transpiration rate; F_v/F_m – maximal quantum efficiency of PSII; g_{H2O} – water vapor conductance; MDA – malondialdehyde; NPQ – nonphotochemical quenching; P_N – net assimilation rate; TAOC – total antioxidant capacity; VPD – air to leaf vapor pressure deficit; Φ_{PSII} – quantum yield of photosynthetic electron transport.

Parameter	Control		Drought	
	Mean	SD	Mean	SD
H_2O_2 [µmol 0.1 ml^{-1}]	73.84	43.39	114.25	67.46
MDA [nmol ml^{-1}]	3.43	1.33	6.04	2.55
TAOC [U 0.1 ml^{-1}]	8.82	8.51	12.71	10.92
E [mmol(H_2O) m^{-2} s^{-1}]	2.05	0.39	0.85	0.39
VPD [Pa kPa^{-1}]	22.49	5.57	27.14	8.88
g_{H2O} [mol(H_2O) m^{-2} s^{-1}]	91.58	35.06	36.73	17.67
P_N [µmol m^{-2}s^{-1}]	10.31	1.87	1.62	0.90
C_i/C_a	0.49	0.09	0.81	0.13
F_v/F_m	0.79	0.02	0.73	0.04
Φ_{PSII}	0.78	0.02	0.70	0.05
NPQ	0.02	0.00	0.03	0.01

was observed in HD-6 and La-posta-seq, respectively (Table 1).

Quantum yield of photosynthetic electron transport (Φ_{PSII}): The Φ_{PSII} was reduced in drought treatment in all genotypes (Fig. 3*B*). Genotype GJ-3 showed a higher yield followed by GJ-14 and the least by HD-6 under control, while in drought, it ranged from La-posta-seq (0.603) to YS-18B-150-43 (0.754). The positive delta change [(C – T)/C], was the lowest in HD-6 followed by JH-19A-501-23 and the highest was observed in La-posta-seq (Table 1).

Nonphotochemical quenching (NPQ): The NPQ increased considerably in all genotypes under drought compared to control (Fig. 3*C*). NPQ was the lowest in JH-19A-501-36 followed by GJ-2 and the highest was in JH-19A-501-23 under control. Under drought, NPQ was the lowest in YS-18B-150-43 followed by JH-19A-501-36, and the highest was observed in JL-118. The lowest and highest positive delta change [(T – C)/C] was seen in JH-19A-501-23 and JL-118, respectively (Table 1).

Quantum yield of NPQ-related energy loss (Y_{NPQ}): The Y_{NPQ} denotes the fraction of energy dissipated in the form of heat *via* the regulated nonphotochemical quenching mechanism. The Y_{NPQ} was higher in all genotypes under drought than that in control (Fig. 3*D*). Genotype YS-18B-501-36 showed the lowest Y_{NPQ} followed by GJ-2 and the highest was observed in JH-19A-501-23 under control. Under drought, genotype YS-18B-150-43 showed the lowest followed by YS-18B-501-36, and the highest was observed in JL-118. The positive delta change [(T – C)/C] was the lowest in YS-18B-150-43 and the highest in JL-118 (Table 1).

Correlation and Principal Component Analysis (PCA): Correlation was performed between traits measured under control (Table 3) and drought (Table 4) to check the pattern of the association.

Under control conditions, TAOC and H_2O_2 were significantly correlated positively (r = 0.77*). Similarly, C_i/C_a and g_{H2O} (r = 0.76**), F_v/F_m and P_N (r = 0.68*), and Φ_{PSII} and F_v/F_m (r = 0.91**) were significantly associated positively. However, H_2O_2 and VPD; C_i/C_a and VPD; g_{H2O} and VPD were significantly negatively correlated. Under drought, H_2O_2 and TAOC (r = 0.78**), MDA and E (r = 0.59*), and g_{H2O} and E (r = 0.78**) were significantly positively correlated, and Φ_{PSII} and NPQ were negatively correlated. Further PCA biplot analysis was performed separately for control (Fig. 4*A*) and drought (Fig. 4*B*). Three principal components for control covered more than 76% of the variation (Table 5) and its biplot showed that MDA and NPQ; H_2O_2 and C_i/C_a; Φ_{PSII}, F_v/F_m, and E; and g_{H2O} and P_N were grouped, while VPD spotted separately, which is mostly influenced by temperature and relative humidity. However, no specific clustering of genotypes was observed under control, suggesting genetic diversity of the genotypes used.

Under drought, three principal components covered 70% of the variation and there were four clusters, cluster 1 (NPQ, VPD), cluster 2 (MDA, g_{H2O}, C_i/C_a), cluster 3 (F_v/F_m, Φ_{PSII}), and P_N spotted separately (Fig. 4*B*). Further, more genotype clusters were seen in the drought biplot, where GJ-3 and JH-19A-501-23; JH-19A-501-36 and GJ-14; La-posta-seq and JL-118; and YS-18B-150-43 and JH-18A-514-38 were clustered, respectively, while HD-6 spotted separately towards F_v/F_m vector. Genotype La-posta-seq was spotted separately in the control biplot, while it clustered together with JL-118 in drought with higher NPQ and VPD. Genotype GJ-3 grouped with JH-19A-501-23 under drought towards E vector, but in control, it was in mid-VPD vector.

The NPQ and MDA showed higher variation in control compared to drought, while F_v/F_m and Φ_{PSII} had greater variation in drought. A higher variation (mean sum of squares) in genotype × environment interaction was observed in H_2O_2, g_{H2O}, VPD, TAOC, and MDA, suggesting that these traits are highly influenced by the drought (Table 6). GJ-2 maintained higher TAOC both in control and drought. Under control HD-6 showed higher E, F_v/F_m, and Φ_{PSII}, while under drought, HD-6 maintained higher photosynthetic efficiency and lower E, making it more drought tolerant. The lower photosynthetic efficiency of genotypes La-posta-seq and JL-118 could be due to higher NPQ and VPD under drought. YS-18B-150-44 was found to be the most stable genotype under both control and drought (near to origin in both biplots). Genotype GJ-14 was stable for both H_2O_2 and C_i/C_a under both control and drought.

Discussion

Drought significantly increases membrane damage and total antioxidant capacity: Hydrogen peroxide, though involved in various signaling processes (Singh *et al.*

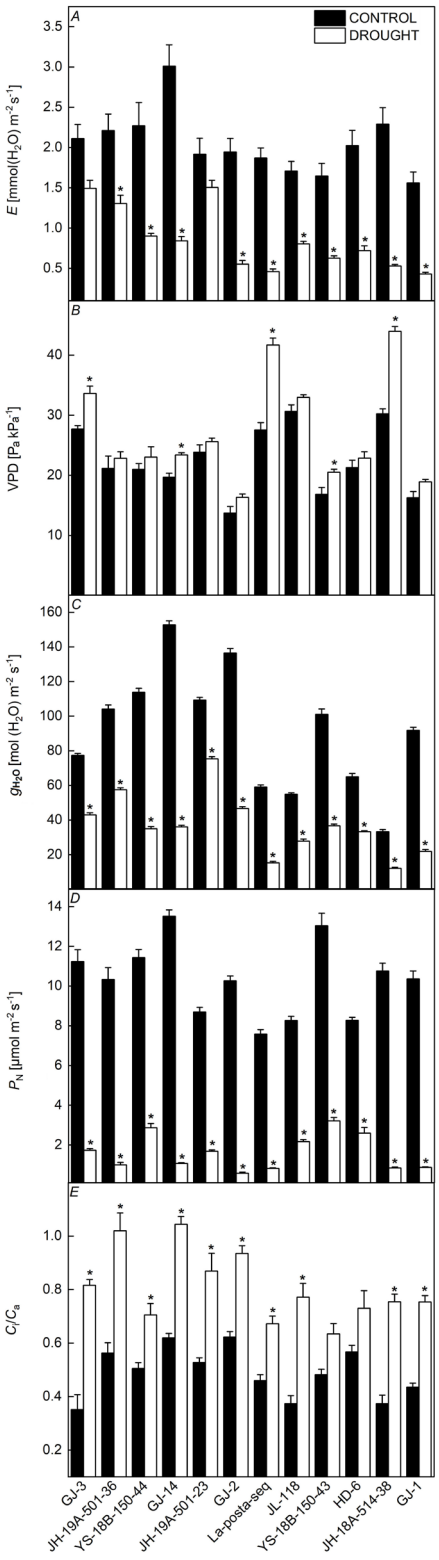

Fig. 2. Gas-exchange parameters of maize seedlings leaves under control and drought stress. (*A*) Transpiration rate (*E*), (*B*) vapour pressure deficit (VPD), (*C*) water vapour conductance (g_{H2O}), (*D*) assimilation rate (P_N), and (*E*) intercellular/ambient CO_2 concentration (C_i/C_a). Values represent means ± SE, n = 5. * indicates significant differences at P<0.05.

2019), becomes toxic and causes damage to cells if it is not scavenged to maintain below damageable level (Dat *et al*. 2000). H_2O_2 increased in all genotypes under drought suggesting stress signal induction and occurrence of drought-induced oxidative stress. It is also supported by a low correlation (r = 0.25) between MDA and H_2O_2 under drought suggesting H_2O_2 is also involved in signal induction in addition to cell membrane damage (Smirnoff and Arnaud 2019). This is supported by GJ-1 and

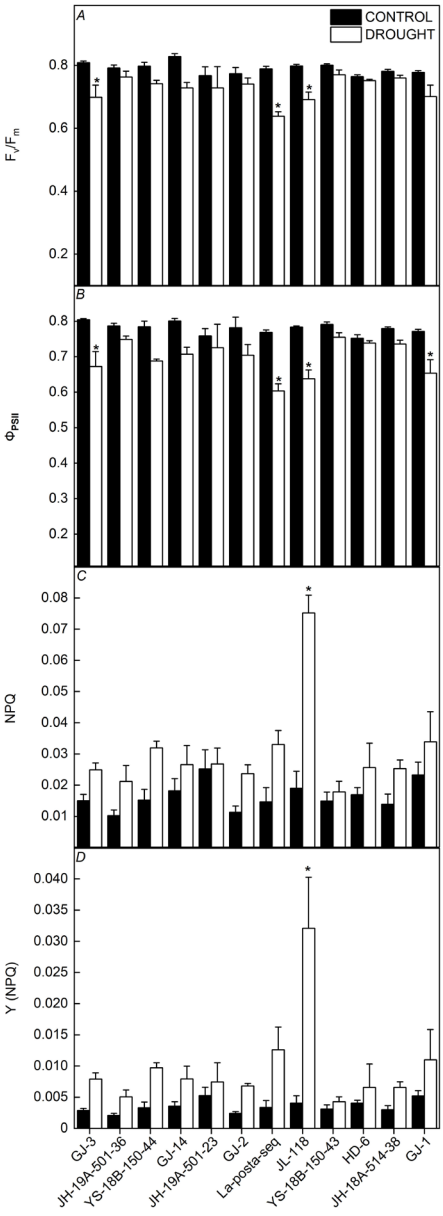

Fig. 3. Chlorophyll fluorescence parameters of maize seedlings leaves under control and drought stress. (*A*) Maximal quantum efficiency of photosystem II (F_v/F_m), (*B*) quantum yield of photosynthetic electron transport (Φ_{PSII}), (*C*) nonphotochemical quenching (NPQ), and (*D*) quantum yield of NPQ-related energy loss (Y_{NPQ}). Values represent means ± SE, n = 5. * indicates significant differences at P<0.05.

Table 3. *Pearson*'s correlation between recorded parameters under control conditions. * Significant at $P<0.05$ and ** significant at $P<0.01$. C_i/C_a – the ratio of intercellular to ambient CO_2 concentration; E – transpiration rate; F_v/F_m – maximal quantum efficiency of PSII; g_{H2O} – water vapor conductance; MDA – malondialdehyde; NPQ – nonphotochemical quenching; P_N – net assimilation rate; TAOC – total antioxidant capacity; VPD – air to leaf vapor pressure deficit; Y_{NPQ} – quantum yield of NPQ-related energy loss; Φ_{PSII} – quantum yield of photosynthetic electron transport.

	H_2O_2	MDA	TAOC	E	VPD	g_{H2O}	P_N	C_i/C_a	F_v/F_m	Φ_{PSII}	NPQ	Y_{NPQ}
H_2O_2	1	0.067	0.768**	0.036	–0.633*	0.539	0.025	0.529	–0.023	–0.120	0.179	0.181
MDA	0.067	1	–0.035	–0.163	–0.131	0.291	0.069	0.108	–0.226	–0.136	0.463	0.353
TAOC	0.768**	–0.035	1	–0.001	–0.442	0.202	–0.133	0.434	–0.217	–0.246	–0.126	–0.057
E	0.036	–0.163	–0.001	1	0.057	0.395	0.483	0.395	0.528	0.418	–0.223	–0.322
VPD	–0.633*	–0.131	–0.442	0.057	1	–0.740**	–0.419	–0.697*	–0.045	–0.005	0.046	0.027
g_{H2O}	0.539	0.291	0.202	0.395	–0.745**	1	0.549	0.762**	0.448	0.328	0.021	–0.087
P_N	0.025	0.069	–0.133	0.483	–0.419	0.549	1	0.170	0.682*	0.748**	–0.193	–0.326
C_i/C_a	0.529	0.108	0.434	0.395	–0.697*	0.762**	0.170	1	0.049	–0.145	–0.145	–0.137
F_v/F_m	–0.023	–0.226	–0.217	0.528	–0.045	0.448	0.682*	0.049	1	0.916**	–0.305	–0.459
Φ_{PSII}	–0.120	–0.136	–0.246	0.418	–0.005	0.328	0.748**	–0.145	0.916**	1	–0.396	–0.564
NPQ	0.179	0.463	–0.126	–0.223	0.046	0.021	–0.193	–0.145	–0.305	–0.396	1	0.973**
Y_{NPQ}	0.181	0.353	–0.057	–0.322	0.027	–0.087	–0.326	–0.137	–0.459	–0.564	0.973**	1

Table 4. *Pearson*'s correlation between recorded parameters under drought. * Significant at $P<0.05$ and ** significant at $P<0.01$. C_i/C_a – the ratio of intercellular to ambient CO_2 concentration; E – transpiration rate; F_v/F_m – maximal quantum efficiency of PSII; g_{H2O} – water vapor conductance; MDA – malondialdehyde; NPQ – nonphotochemical quenching; P_N – net assimilation rate; TAOC – total antioxidant capacity; VPD – air to leaf vapor pressure deficit; Y_{NPQ} – quantum yield of NPQ-related energy loss; Φ_{PSII} – quantum yield of photosynthetic electron transport.

	H_2O_2	MDA	TAOC	E	VPD	g_{H2O}	P_N	C_i/C_a	F_v/F_m	Φ_{PSII}	NPQ	Y_{NPQ}
H_2O_2	1	0.250	0.782**	–0.050	–0.304	0.158	–0.428	0.383	–0.102	–0.070	–0.220	–0.205
MDA	0.250	1	0.136	0.595*	–0.198	0.463	0.254	0.037	0.055	0.135	–0.361	–0.335
TAOC	0.782**	0.136	1	–0.028	–0.308	0.089	–0.007	0.141	0.160	0.183	–0.291	–0.296
E	–0.050	0.595*	–0.028	1	–0.042	0.785**	0.149	0.426	0.122	0.249	–0.119	–0.126
VPD	–0.304	–0.198	–0.308	–0.042	1	–0.490	–0.209	–0.305	–0.451	–0.377	0.261	0.289
g_{H2O}	0.158	0.463	0.089	0.785**	–0.490	1	0.096	0.533	0.330	0.451	–0.276	–0.289
P_N	–0.428	0.254	–0.007	0.149	–0.209	0.096	1	–0.533	0.310	0.254	0.103	0.086
C_i/C_a	0.383	0.037	0.141	0.426	–0.305	0.533	–0.533	1	0.210	0.268	–0.161	–0.171
F_v/F_m	–0.102	0.055	0.160	0.122	–0.451	0.330	0.310	0.210	1	0.949**	–0.487	–0.541
Φ_{PSII}	–0.070	0.135	0.183	0.249	–0.377	0.451	0.254	0.268	0.949**	1	–0.606*	–0.649*
NPQ	–0.220	–0.361	–0.291	–0.119	0.261	–0.276	0.103	–0.161	–0.487	–0.606*	1	0.995**
Y_{NPQ}	–0.205	–0.335	–0.296	–0.126	0.289	–0.289	0.086	–0.171	–0.541	–0.649*	0.995**	1

JH-19A-501-36 which showed a minute increase in H_2O_2 content in drought compared to control, thus ranking first and second respectively for H_2O_2 production and scavenging. However, MDA was higher in GJ-1 under drought though it showed a marginal increase of H_2O_2 under drought compared to control, while GJ-3 showed a significant increase in both H_2O_2 and MDA under drought compared to control (Fig. 1*A*,*C*). An increase in H_2O_2 content damages the cell membrane by reacting with lipids and proteins causing lipid peroxidation. MDA content indicates the level of lipid peroxidation and membrane damage (Porcel and Ruiz-Lozano 2004, Abid *et al.* 2018) but MDA content under drought is more positively associated with water loss (transpiration rate) ($r = 0.595^*$) (Table 4), indicating stomatal closure is a drought-adaptive mechanism (Cornic 2000). Likewise, a study on *Eugenia uniflora* L. also showed a strong correlation between MDA and E under water stress (Toscano *et al.* 2016).

Further, TAOC and H_2O_2 had a significantly higher correlation both under control and drought suggesting that as H_2O_2 increased, total antioxidants also increased to scavenge them. Likewise, Anjum *et al.* (2017) reported that drought stress increased H_2O_2, $O_2^{\cdot-}$, and MDA compared to well-watered maize hybrids, and there was also increased activity of various enzymatic and nonenzymatic antioxidant activities under drought. Similarly, drought tolerance was associated with increased antioxidants and redox-regulating enzymes [catalase (CAT), ascorbate peroxidase (APX), glutathione reductase (GR), and glutathione peroxidase (GPX)] in maize (Avramova *et al.*

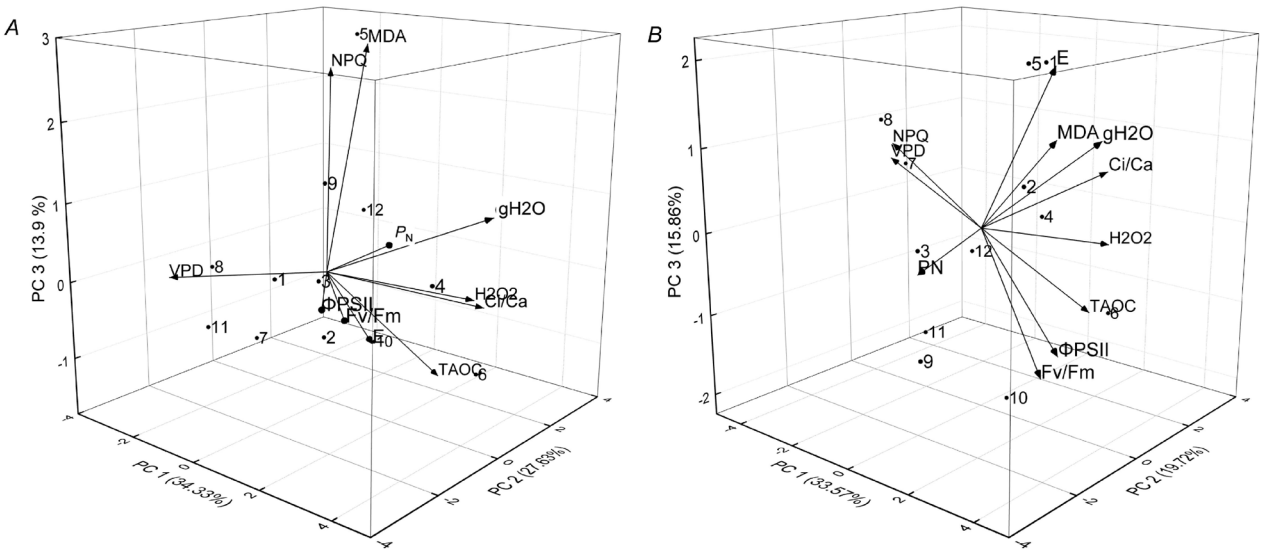

Fig. 4. Principal component (PC) biplot analysis of recorded parameters [hydrogen peroxide (H_2O_2), total antioxidant capacity (TAOC), malondialdehyde (MDA) content, transpiration rate (*E*), vapour pressure deficit (VPD), water vapour conductance (g_{H2O}), assimilation rate (P_N), intercellular/ambient CO_2 concentration (C_i/C_a), maximal quantum efficiency of photosystem II (F_v/F_m), quantum yield of photosynthetic electron transport (Φ_{PSII}), and nonphotochemical quenching (NPQ)] and genotypes [1 – GJ-3, 2 – JH-19A-501-36, 3 – YS-18B-150-44, 4 – GJ-14, 5 – JH-19A-501-23, 6 – GJ-2, 7 – La-posta-seq, 8 – JL-118, 9 – YS-18B-150-43, 10 – HD-6, 11– JH-18A-514-38, 12 – GJ-1] under control (*A*) and drought (*B*).

Table 5. Principal component (PC) analysis and percentage [%] variance coverage under control and drought.

PC	Control			Drought		
	Eigenvalue	Variance [%]	Cumulative [%]	Eigenvalue	Variance [%]	Cumulative [%]
1	3.7762	34.33	34.33	3.6932	33.57	33.57
2	3.0398	27.63	61.96	2.1691	19.72	53.29
3	1.5319	13.93	75.89	1.7450	15.86	69.16
4	0.8726	7.93	83.82	1.3644	12.40	81.56
5	0.7536	6.85	90.67	0.9394	8.54	90.10
6	0.5319	4.83	95.51	0.5860	5.33	95.43
7	0.3484	3.17	98.68	0.2693	2.45	97.88
8	0.0919	0.84	99.51	0.1521	1.38	99.26
9	0.0382	0.35	99.86	0.0583	0.53	99.79
10	0.0127	0.12	99.97	0.0206	0.19	99.98
11	0.0028	0.03	100.00	0.0027	0.02	100.00

Table 6. Mean sum of the square of all traits due to environment, genotype, and their interaction. C_i/C_a – the ratio of intercellular to ambient CO_2 concentration; *E* – transpiration rate; F_v/F_m – maximal quantum efficiency of PSII; g_{H2O} – water vapor conductance; MDA – malondialdehyde; NPQ – nonphotochemical quenching; P_N – net assimilation rate; TAOC – total antioxidant capacity; VPD – air to leaf vapor pressure deficit; Y_{NPQ} – quantum yield of NPQ-related energy loss; Φ_{PSII} – quantum yield of photosynthetic electron transport.

	H_2O_2	MDA	TAOC	*E*	P_N	g_{H2O}	VPD	C_i/C_a	F_v/F_m	Φ_{PSII}	NPQ	Y_{NPQ}
Environment	32,431.29	134.459	294.100	25.974	1,385.66	54,645.43	383.507	1.866	0.089	0.153	0.004	8.32×10^{-4}
Genotype	20,941.48	20.325	690.262	0.530	7.83	3,332.77	298.005	0.057	0.003	0.006	7.30×10^{-4}	1.72×10^{-4}
Interaction	2,113.90	6.006	18.983	0.339	6.13	1,287.62	30.120	0.018	0.004	0.005	5.06×10^{-4}	1.45×10^{-4}

2017). Concerning MDA and TAOC, HD-6 showed lower MDA and higher TAOC increase in drought from control. However, in the present study, no significant negative correlation between MDA and TAOC was observed, which could be due to the operation of other membrane damaging substances other than ROS produced under drought or

disruption of the ROS-scavenging system under severe drought (Sharma *et al.* 2012). Based on the H_2O_2 content, MDA, and total antioxidant content, HD-6 was observed to have a good balance of H_2O_2 and lower cell membrane damage under drought. However, JH-19A-501-23 had the lowest MDA delta change, but showed less TAOC. Further, with respect to MDA and H_2O_2 content, GJ-3 was found to be susceptible to drought stress.

Severe drought stress imposes both stomatal and non-stomatal limitations on photosynthesis: ROS are well-known causes of damage to photosystems of the plant (Khorobrykh *et al.* 2020). In the present study, the negative association of the assimilation rate with H_2O_2 (r = –0.43) and C_i/C_a (r = –0.53) under drought (Table 4) could be due to disruption of D1 proteins of PSII by ROS (Mishra and Ghanotakis 1994, Miyao *et al.* 1995). The D1 protein is the main subunit of PSII (Barber *et al.* 1997) and is directly involved in photosynthetic electron transport (Edelman and Mattoo 2008). In HD-6 and JL-118, P_N is reduced by fewer units in drought compared to other genotypes from their respective control (Fig. 2*D*). The VPD, which is measured by the difference between water vapor pressure in the leaf and the water vapor pressure of the ambient air, gives an accurate idea of leaf water balance (Grossiord *et al.* 2020). Both genotypes HD-6 and JH-19A-501-23 showed relatively less delta change for VPD suggesting only a marginal increase of VPD in drought compared to control. An increase in VPD makes stomata smaller and reduces stomatal conductance to save water and limit photosynthesis (Grossiord *et al.* 2020). La-post-seq and JH-19A-514-38 showed significantly higher VPD and accordingly their P_N was the lowest among all genotypes under drought (Fig. 2*B*,*D*). Further, VPD had a negative correlation (r = –0.21) with P_N under drought (Table 4). The photosynthetic rate is limited by both stomatal and nonstomatal limitations (Cossins and Chen 1997). During the initiation of drought or under mild to moderate drought stress, the decline in photosynthesis occurs mostly due to a reduction in the internal cellular CO_2 concentration by stomatal closure (Lawlor 2002). However nonstomatal limitations also reduce photosynthesis due to impaired metabolic processes, such as RuBP synthesis, ATP synthesis, and electron transfer (Cossins and Chen 1997). In the present study, C_i/C_a ratio significantly increased in all genotypes under drought stress, though there was a reduction in stomatal conductance. Similar increases in C_i/C_a ratio under severe drought were previously reported in rice (Ji *et al.* 2012), maize (Zhang *et al.* 2015), cowpea (Singh and Reddy 2011), and wheat (Martin and Ruiz-Torres 1992). Genotype HD-6 showed the lowest delta change with a marginal increase in internal CO_2 concentration under drought compared to control suggesting nonstomatal limitation was relatively lesser in HD-6 compared to others. The highest C_i/C_a delta change of GJ-3 could be due to pronounced production of H_2O_2 and higher MDA content under drought compared to control (Table 1). Further, C_i/C_a showed a positive correlation (r = 0.38) with H_2O_2 and g_{H2O} (r = 0.53) suggesting that water loss increases drought stress and thus enhances H_2O_2 production.

Concerning g_{H2O}, JH-19A-501-23 and GJ-3 showed lesser delta change. Drought stress usually reduces stomatal conductance and transpiration to save water, which reduces the CO_2 influx, thus reducing the final photosynthetic assimilation (Oukarroum *et al.* 2009, Pinheiro and Chaves 2011). The delta change of transpiration rate was also the lowest in JH-19A-501-23 and GJ-3 suggesting that under drought, the transpiration rate of JH-19A-501-23 did not compromise lot and it's P_N [(C – T/C)] was also comparatively higher (Table 1). Overall, based on gas-exchange parameters, genotypes HD-6 and JH-19A-501-23 were found to be more tolerant than other genotypes.

Drought disrupts photosynthesis and tolerant genotype (HD-6) shows comparatively higher PSII photochemical efficiency: Chl fluorescence provides detailed information on the state of PSII and its response to environmental change (Murchie and Lawson 2013). The F_v/F_m ratio denotes maximal photochemical efficiency of PSII reaction centers (Butler 1978) and low F_v/F_m implies underutilization of light energy absorbed by PSII reaction centers (Fracheboud and Leipner 2003).

F_v/F_m negatively correlated with VPD (r = –0.45) suggesting high VPD may reduce photosynthetic efficiency under drought stress. A larger value of VPD was associated with a reduction in stomatal conductance (Dos Santos *et al.* 2017) and thus reduced photosynthesis (Shirke and Pathre 2004). Under drought, HD-6 showed only marginal reduction in F_v/F_m (0.751) compared to its respective control (0.764) (Fig. 3*A*, Table 1) implying relatively higher photosynthetic efficiency in HD-6 under drought. The delta change of F_v/F_m was also lowest for HD-6. However, in JH-19A-501-23, F_v/F_m ratio declined by 0.05 in drought compared to the control.

The Φ_{PSII}, effective PSII quantum yield, denotes the fraction of absorbed energy used in photochemistry, which determines the efficiency of PSII (Tsai *et al.* 2019). It tells the proportion of the light used in PSII photochemistry (Murata 1992). It is affected by the rate of electron transport or the concentrations of electron acceptors, *e.g.*, $NADP^+$, available at the acceptor side of PSI (Tsai *et al.* 2019). F_v/F_m showed a significantly high positive correlation (r = –0.95**) with Φ_{PSII}. Genotypes HD-6 and JH-19A-501-23 showed a relatively low decline in the Φ_{PSII} under drought compared to other genotypes (Fig. 3*B*, Table 1).

Nonphotochemical quenching (NPQ) is widely used to measure the nonradiative energy dissipation (Bilger and Björkman 1990). The surplus fraction of the absorbed light is dissipated as heat known as NPQ (Chen *et al.* 2019). Drought stress not only damages PSII but also the light-harvesting complex (Hura *et al.* 2007). NPQ is one of the strategies adopted by plants to mitigate damage by harmlessly quenching the excitation of chlorophyll within the light-harvesting antennae of PSII by converting excitation energy into thermal energy, which can then

be released (Kasajima *et al.* 2011), thus reducing the formation of free radicals. Likewise in the present study, under control conditions, NPQ positively correlated with MDA, but under drought, it was negatively correlated with H_2O_2 (r = –0.22) and MDA (r = –0.36) (Table 5). Further, NPQ is negatively associated with Φ_{PSII} (–0.606*) under drought, which could be due to NPQ-led downregulation of photosynthesis (Murchie and Lawson 2013) by competing with photochemistry for the absorbed energy (Bilger and Björkman 1990). In JH-19A-501-23, NPQ increased marginally under drought (1.06 times) compared to other genotypes (Fig. 3*C*), whereas in JL-118 under drought, NPQ increased around 4 times compared to control, implying comparatively less photosystem damage and downregulation of photosynthesis in JH-19A-501-23 under drought. However, in HD-6, under drought, NPQ increased 1.5 times compared to control. The Y_{NPQ} also decreased marginally under drought in YS-18B-150-43, JH-19A-501-23, and HD-6 compared to control. Y_{NPQ} denotes the fraction of energy dissipated in the form of heat *via* the regulated nonphotochemical quenching mechanism (Huang *et al.* 2012) and it also showed a negative correlation with Φ_{PSII} (r = –0.65*).

Overall, based on biochemical, gas exchange, and chlorophyll fluorescence parameters, HD-6 performed well under drought followed by JH-19A-501-23.

Principal component analysis and genotype × environment interaction: PCA for measured parameters under control revealed that H_2O_2 and C_i/C_a clustered together, suggesting that internal CO_2 influences H_2O_2 accumulation. Higher CO_2 concentration in soybean was reported to have accumulated higher H_2O_2 in leaf tissues (Cheeseman 2006). Further, E, F_v/F_m, and Φ_{PSII} interact and influence CO_2 assimilation and photosynthetic efficiency, while MDA accumulation could increase NPQ to remove excess light as heat. Previous studies have found that mutants lacking the capacity to induce NPQ are very sensitive to photoinhibition and drought stress (Cousins *et al*. 2002, Allorent *et al.* 2013).

However, under drought, clustering of MDA, g_{H2O}, C_i/C_a, and E (Fig. 4*B*) suggests that higher stomatal conductance and transpiration increase membrane damage which finally leads to a collapse of photosystems (shown by the increase in C_i). Further, VPD increases NPQ (grouped together) to remove excess heat and save the plant from photoinhibition, while under control, VPD is spotted alone in the control biplot. The assimilation rate was less influenced by other factors under drought suggesting the operation of other unmeasured processes. Furthermore, biplot analysis under control and drought showed that genotypes behaved differently in these two conditions. More elaborately, HD-6 had higher photosynthetic efficiency in drought, but under control, it was more aligned towards E (Fig. 4*A*), suggesting that increasing photosynthetic efficiency and reducing transpiration rate could be a better tolerance mechanism under drought. Supporting this, GJ-3, which was spotted near MDA and NPQ vectors in control, was shown to have a higher transpiration rate thus having reduced photosynthetic efficiency and being relatively susceptible. A higher genotype × environment interaction, the mean sum of the square of H_2O_2, g_{H2O}, VPD, TAOC, and MDA (Table 6), suggests that these traits are highly influenced by the drought; thus, these traits may be important when selecting for drought-tolerant genotypes. Based on all measured parameters, HD-6 genotype performed well, with higher TAOC and the lower decrease in P_N and photosynthetic efficiency under drought compared to control.

Conclusion: Plants under drought stress responded through complex processes and interactions. Drought increased the generation of ROS and caused lipid peroxidation. Drought-tolerant genotypes balance the ROS by producing a higher amount of antioxidants to scavenge them thus reducing cell damage. CO_2 assimilation rate was reduced by both stomatal and nonstomatal inhibition of photosynthesis under severe drought stress. An increase in transpiration rate was found to increase MDA content under drought. Likewise, MDA, E, g_{H2O}, and C_i/C_a clustered together in PCA analysis showing their strong interactions. However, the assimilation rate associated with g_{H2O} under control conditions, but under drought, it was located separately in PCA, suggesting some other factors involved in increasing the assimilation rate under drought. Correlation analysis showed that assimilation rate was negatively associated with H_2O_2 and C_i content under drought, implying that imbalance of ROS impairs and inhibits photosystems. Similarly, MDA was positively associated with NPQ in control, while under drought, MDA was strongly influenced by g_{H2O}, rather than NPQ. Thus looking for variation with higher stomatal adjustment, lower H_2O_2 content and lesser C_i under severe drought could able to identify drought-tolerant donors in maize. Further, reducing transpiration rate and increasing photosynthetic efficiency (F_v/F_m) under drought would be a better drought-adaptation mechanism for maize. Based on biochemical and photosynthetic parameters, HD-6 was observed to be more tolerant against severe drought stress and behaved differently than other genotypes. The holistic and multi-omics approach could reveal more information on the interaction of biochemical and photosynthetic parameters.

References

Abid M., Ali S., Qi L.K. *et al.*: Physiological and biochemical changes during drought and recovery periods at tillering and jointing stages in wheat (*Triticum aestivum* L.). – Sci. Rep.-UK **8**: 4615, 2018.

Allorent G., Tokutsu R., Roach T. *et al.*: A dual strategy to cope with high light in *Chlamydomonas reinhardtii*. – Plant Cell **25**: 545-557, 2013.

Anjum S.A., Ashraf U., Tanveer M. *et al.*: Drought induced changes in growth, osmolyte accumulation and antioxidant metabolism of three maize hybrids. – Front. Plant Sci. **8**: 69, 2017.

Apel K., Hirt H.: Reactive oxygen species: Metabolism, oxidative stress, and signal transduction. – Annu. Rev. Plant Biol. **55**: 373-399, 2004.

Asada K.: The water-water cycle in chloroplasts: Scavenging of active oxygens and dissipation of excess photons. – Annu. Rev. Plant Biol. **50**: 601-639, 1999.

Asada K., Takahashi M.: Production and scavenging of active oxygen in photosynthesis. – In: Kyle D.J., Osmond C.B., Arntzen C.J. (ed.): Photoinhibition. Topics in Photosynthesis. Vol. 9. Pp. 227-287. Elsevier, Amsterdam 1987.

Assefa F., Ayalew D.: Status and control measures of fall armyworm (*Spodoptera frugiperda*) infestations in maize fields in Ethiopia: A review. – Cogent Food Agric. **5**: 1641902, 2019.

Avramova V., AbdElgawad H., Vasileva I. *et al.*: High antioxidant activity facilitates maintenance of cell division in leaves of drought tolerant maize hybrids. – Front. Plant Sci. **8**: 84, 2017.

Baker N.R.: Chlorophyll fluorescence: A probe of photosynthesis *in vivo*. – Annu. Rev. Plant Biol. **59**: 89-113, 2008.

Barber J., Nield J., Morris E.P. *et al.*: The structure, function and dynamics of photosystem two. – Physiol. Plantarum **100**: 817-827, 1997.

Bhaskara G.B., Nguyen T.T., Verslues P.E.: Unique drought resistance functions of the *Highly ABA-induced* clade A protein phosphatase 2Cs. – Plant Physiol. **160**: 379-395, 2012.

Bilger W., Björkman O.: Role of the xanthophyll cycle in photoprotection elucidated by measurements of light-induced absorbance changes, fluorescence and photosynthesis in leaves of *Hedera canariensis*. – Photosynth. Res. **25**: 173-185, 1990.

Boo Y.C., Jung J.: Water deficit-induced oxidative stress and antioxidative defenses in rice plants. – J. Plant Physiol. **155**: 255-261, 1999.

Butler W.L.: Energy distribution in the photochemical apparatus of photosynthesis. – Annu. Rev. Plant Physiol. **29**: 345-378, 1978.

Cheeseman J.M.: Hydrogen peroxide concentrations in leaves under natural conditions. – J. Exp. Bot. **57**: 2435-2444, 2006.

Chen X., Mo X., Hu S. *et al.*: Relationship between fluorescence yield and photochemical yield under water stress and intermediate light conditions. – J. Exp. Bot. **70**: 301-313, 2019.

Cornic G.: Drought stress inhibits photosynthesis by decreasing stomatal aperture – not by affecting ATP synthesis. – Trends Plant Sci. **5**: 187-188, 2000.

Cossins E.A., Chen L.: Folates and one-carbon metabolism in plants and fungi. – Phytochemistry **45**: 437-452, 1997.

Cousins A.B., Adam N.R., Wall G.W. *et al.*: Photosystem II energy use, non-photochemical quenching and the xanthophyll cycle in *Sorghum bicolor* grown under drought and free-air CO_2 enrichment (FACE) conditions. – Plant Cell Environ. **25**: 1551-1559, 2002.

Cruz de Carvalho M.H.: Drought stress and reactive oxygen species: Production, scavenging and signaling. – Plant Signal. Behav. **3**: 156-165, 2008.

Dat J., Vandenabeele S., Vranová E. *et al.*: Dual action of the active oxygen species during plant stress responses. – Cell Mol. Life Sci **57**: 779-795, 2000.

Davies W.J., Zhang J.: Root signals and the regulation of growth and development of plants in drying soil. – Annu. Rev. Plant Phys. **42**: 55-76, 1991.

Dhindsa R.S., Plumb-Dhindsa P., Thorpe T.A.: Leaf senescence: Correlated with increased levels of membrane permeability and lipid peroxidation, and decreased levels of superoxide dismutase and catalase. – J. Exp. Bot. **32**: 93-101, 1981.

Dos Santos C.M., Endres L., Ferreira V.M. *et al.*: Photosynthetic capacity and water use efficiency in *Ricinus communis* (L.) under drought stress in semi-humid and semi-arid areas. – An. Acad. Bras. Ciênc. **89**: 3015-3029, 2017.

Edelman M., Mattoo A.K.: D1-protein dynamics in photosystem II: The lingering enigma. – Photosynth. Res. **98**: 609-620, 2008.

Farooq M., Wahid A., Kobayashi N. *et al.*: Plant drought stress: effects, mechanisms and management. – Agron. Sustain. Dev. **29**: 185-212, 2009.

Farré I., van Oijen M., Leffelaar P.A., Faci J.M.: Analysis of maize growth for different irrigation strategies in northeastern Spain. – Eur. J. Agron. **12**: 225-238, 2000.

Fisher M., Abate T., Lunduka R.W. *et al.*: Drought tolerant maize for farmer adaptation to drought in sub-Saharan Africa: Determinants of adoption in eastern and southern Africa. – Climatic Change **133**: 283-299, 2015.

Fracheboud Y., Leipner J.: The application of chlorophyll fluorescence to study light, temperature, and drought stress. – In: DeEll J.R., Toivonen P.M.A. (ed.): Practical Applications of Chlorophyll Fluorescence in Plant Biology. Pp. 125-150. Springer, Boston 2003.

Genty B., Briantais J.-M., Baker N.R.: The relationship between the quantum yield of photosynthetic electron transport and quenching of chlorophyll fluorescence. – BBA-Gen. Subjects **990**: 87-92, 1989.

Gill S.S., Tuteja N.: Reactive oxygen species and antioxidant machinery in abiotic stress tolerance in crop plants. – Plant Physiol. Bioch. **48**: 909-930, 2010.

Grossiord C., Buckley T.N., Cernusak L.A. *et al.*: Plant responses to rising vapor pressure deficit. – New Phytol. **226**: 1550-1566, 2020.

Huang W., Zhang S.B., Cao K.F.: Evidence for leaf fold to remedy the deficiency of physiological photoprotection for photosystem II. – Photosynth. Res. **110**: 185-191, 2012.

Hura T., Hura K., Grzesiak M., Rzepka A.: Effect of long-term drought stress on leaf gas exchange and fluorescence parameters in C_3 and C_4 plants. – Acta Physiol. Plant. **29**: 103, 2007.

Jakob B., Heber U.: Photoproduction and detoxification of hydroxyl radicals in chloroplasts and leaves and relation to photoinactivation of photosystems I and II. – Plant Cell Physiol. **37**: 629-635, 1996.

Ji K., Wang Y., Sun W. *et al.*: Drought-responsive mechanisms in rice genotypes with contrasting drought tolerance during reproductive stage. – J. Plant Physiol. **169**: 336-344, 2012.

Kasajima I., Ebana K., Yamamoto T. Uchimiya H.: Molecular distinction in genetic regulation of nonphotochemical quenching in rice. – P. Natl. Acad. Sci. USA **108**: 13835-13840, 2011.

Khorobrykh S., Havurinne V., Mattila H., Tyystjärvi E.: Oxygen and ROS in photosynthesis. – Plants-Basel **9**: 91, 2020.

Kirkham M.B.: Field capacity, wilting point, available water, and the non-limiting water range. – In: Kirkham M.B. (ed.): Principles of Soil and Plant Water Relations. Pp. 101-115. Academic Press, San Diego 2005.

Krause G.H., Weis E.: Chlorophyll fluorescence and photosynthesis: the basics. – Annu. Rev. Plant Phys. **42**: 313-349, 1991.

Heath R.L., Packer L.: Photoperoxidation in isolated chloroplasts: I. Kinetics and stoichiometry of fatty acid peroxidation. – Arch. Biochem. Biophys. **125**: 189-198, 1968.

Lawlor D.W.: Limitation to photosynthesis in water-stressed leaves: Stomata *vs.* metabolism and the role of ATP. – Ann. Bot.-London **89**: 871-885, 2002.

Martin B., Ruiz-Torres N.A.: Effects of water-deficit stress on photosynthesis, its components and component limitations, and on water use efficiency in wheat (*Triticum aestivum* L.). – Plant Physiol. **100**: 733-739, 1992.

Mattos L.M., Moretti C.L.: Oxidative stress in plants under drought conditions and the role of different enzymes. –

Enzym. Eng. **5**: 136, 2015.
Mehler A.H.: Studies on reactions of illuminated chloroplasts: I. Mechanism of the reduction of oxygen and other Hill reagents. – Arch. Biochem. Biophys. **33**: 65-77, 1951.
Mishra N.P., Ghanotakis D.F.: Exposure of photosystem II complex to chemically generated singlet oxygen results in D1 fragments similar to the ones observed during aerobic photoinhibition. – BBA-Bioenergetics **1187**: 296-300, 1994.
Mittler R., Vanderauwera S., Gollery M., Van Breusegem F.: Reactive oxygen gene network of plants. – Trends Plant Sci. **9**: 490-498, 2004.
Miyao M., Ikeuchi M., Yamamoto N., Ono T.: Specific degradation of the D1 protein of photosystem II by treatment with hydrogen peroxide in darkness: implications for the mechanism of degradation of the D1 protein under illumination. – Biochemistry **34**: 10019-10026, 1995.
Murata N. (ed.): Research in Photosynthesis. Pp. 3515. Springer, Dordrecht 1992.
Murchie E.H., Lawson T.: Chlorophyll fluorescence analysis: A guide to good practice and understanding some new applications. – J. Exp. Bot. **64**: 3983-3998, 2013.
Noctor G., Foyer C.H.: Ascorbate and glutathione: Keeping active oxygen under control. – Annu. Rev. Plant Biol. **49**: 249-279, 1998.
Noctor G., Mhamdi A., Foyer C.H.: The roles of reactive oxygen metabolism in drought: Not so cut and dried. – Plant Physiol. **164**: 1636-1648, 2014.
Oukarroum A., Schansker G., Strasser R.J.: Drought stress effects on photosystem I content and photosystem II thermotolerance analyzed using Chl *a* fluorescence kinetics in barley varieties differing in their drought tolerance. – Physiol. Plantarum **137**: 188-199, 2009.
Pinheiro C., Chaves M.M.: Photosynthesis and drought: Can we make metabolic connections from available data? – J. Exp. Bot. **62**: 869-882, 2011.
Polle A.: Dissecting the superoxide dismutase-ascorbate-glutathione-pathway in chloroplasts by metabolic modeling. Computer simulations as a step towards flux analysis. – Plant Physiol. **126**: 445-462, 2001.
Porcel R., Ruiz-Lozano J.M.: Arbuscular mycorrhizal influence on leaf water potential, solute accumulation, and oxidative stress in soybean plants subjected to drought stress. – J. Exp. Bot. **55**: 1743-1750, 2004.
Praba M.L., Cairns J.E., Babu R.C., Lafitte H.R.: Identification of physiological traits underlying cultivar differences in drought tolerance in rice and wheat. – J. Agron. Crop Sci. **195**: 30-46, 2009.
Richter C., Schweizer M.: Oxidative stress in mitochondria. – In: Scandalios J.G. (ed.): Oxidative Stress and the Molecular Biology of Antioxidant Defenses. Pp. 169-200. Cold Spring Harbor Laboratory Press, Plainview 1997.
Sage R.F.: Acclimation of photosynthesis to increasing atmospheric CO_2: The gas exchange perspective. – Photosynth. Res. **39**: 351-368, 1994.
Sgherri C.L.M., Pinzino C., Navari-Izzo F.: Chemical changes and $O_2^{\bullet-}$ production in thylakoid membranes under water stress. – Physiol. Plantarum **87**: 211-216, 1993.
Sharma P., Jha A.B., Dubey R.S., Pessarakli M.: Reactive oxygen species, oxidative damage, and antioxidative defense mechanism in plants under stressful conditions. – J. Bot. **2012**: 217037, 2012.
Shirke P.A., Pathre U.V.: Influence of leaf-to-air vapour pressure deficit (VPD) on the biochemistry and physiology of photosynthesis in *Prosopis juliflora*. – J. Exp. Bot. **55**: 2111-2120, 2004.
Sinclair T.R., Bennett J.M., Muchow R.C.: Relative sensitivity of grain yield and biomass accumulation to drought in field-grown maize. – Crop Sci. **30**: 690-693, 1990.
Singh A., Kumar A., Yadav S. *et al.*: Reactive oxygen species-mediated signaling during abiotic stress. – Plant Gene **18**: 100173, 2019.
Singh S.K., Reddy K.R.: Regulation of photosynthesis, fluorescence, stomatal conductance and water-use efficiency of cowpea (*Vigna unguiculata* [L.] Walp.) under drought. – J. Photoch. Photobio. B **105**: 40-50, 2011.
Smirnoff N.: The role of active oxygen in the response of plants to water deficit and desiccation. – New Phytol. **125**: 27-58, 1993.
Smirnoff N., Arnaud D.: Hydrogen peroxide metabolism and functions in plants. – New Phytol. **221**: 1197-1214, 2019.
Toscano S., Farieri E., Ferrante A., Romano D.: Physiological and biochemical responses in two ornamental shrubs to drought stress. – Front. Plant Sci. **7**: 645, 2016.
Tsai Y.C., Chen K.C., Cheng T.S. *et al.*: Chlorophyll fluorescence analysis in diverse rice varieties reveals the positive correlation between the seedlings salt tolerance and photosynthetic efficiency. – BMC Plant Biol. **19**: 403, 2019.
Tsukagoshi H., Busch W., Benfey P.N.: Transcriptional regulation of ROS controls transition from proliferation to differentiation in the root. – Cell **143**: 606-616, 2010.
von Caemmerer S., Farquhar G.D.: Some relationships between the biochemistry of photosynthesis and the gas exchange of leaves. – Planta **153**: 376-387, 1981.
Veihmeyer F.J., Hendrickson A.H.: The moisture equivalent as a measure of the field capacity of soils. – Soil Sci. **32**: 181-194, 1931.
Zhang J., Davies W.J.: Increased synthesis of ABA in partially dehydrated root tips and ABA transport from roots to leaves. – J. Exp. Bot. **38**: 2015-2023, 1987.
Zhang R.H., Zhang X.H., Camberato J.J., Xue J.Q.: Photosynthetic performance of maize hybrids to drought stress. – Russ. J. Plant Physiol. **62**: 788-796, 2015.
Zipper S.C., Qiu J., Kucharik C.J.: Drought effects on US maize and soybean production: Spatiotemporal patterns and historical changes. – Environ. Res. Lett. **11**: 094021, 2016.